Redox Catalysis

Deutsche Ausgabe: DOI: 10.1002/ange.201601887
Internationale Ausgabe: DOI: 10.1002/anie.201601887

Catalytic Radical Reduction in Aqueous Solution by a Ruthenium Hydride Intermediate

*Yamin Htet and Andrew G. Tennyson**

In memory of Gregory E. Tennyson

Abstract: *Some manganese complexes can catalyze both antioxidant and pro-oxidant reactions, whereby the disparate reactivity modes are determined by the catalyst environment and afford distinct therapeutic effects. We recently reported the reduction of radicals in buffered aqueous solution catalyzed by a ruthenium complex with biologically relevant non-tertiary alcohols as terminal reductants. Mechanistic evidence is presented, indicating that this catalytic radical reduction is achieved by a Ru-hydride intermediate formed by β-hydride elimination from a Ru-alkoxide species. A similar mechanism and Ru-hydride intermediate was previously reported to kill cancer cells with catalytic pro-oxidant effects. Therefore, our demonstration of catalytic antioxidant effects by the same type of intermediate reveals new potential therapeutic strategies and applications for catalytic systems that form Ru-hydride intermediates.*

Reactive oxygen species (ROS) and other free radicals can damage critical biomolecules in living systems and are implicated in a wide variety of pathologies.[1] Antioxidants can reduce ROS or oxidizing radicals and thus protect against damage, but they typically proceed through stoichiometric reductions that deplete their protective capacity.[2] However, a catalytic reduction could regenerate an antioxidant after each turnover and thus enable it to provide significantly greater protection. Manganese porphyrin-based complexes can catalyze $O_2^{\bullet-}$ and H_2O_2 disproportionation reactions and have shown beneficial antioxidant effects in stroke and diabetes therapy by reducing ROS levels.[3] Interestingly, some of these Mn complexes (two of which are in Phase 1 clinical trials) can also produce pro-oxidant effects in cancer cells, which endows them with potent chemotherapeutic activity.[3,4] The ability of a Mn complex to produce antioxidant or pro-oxidant effects in different environments is derived from the same catalytic cycle and intermediates, whereby the catalyst environment determines the antioxidant/pro-oxidant outcome.[3–5] Knowledge of the mechanism and intermediates by which a complex catalyzes a redox reaction in a biological system is thus essential for developing its therapeutic applications.

We recently reported the **Ru1**-catalzyed reduction of $ABTS^{\bullet-}$ into $ABTS^{2-}$ in buffered aqueous solution with biologically relevant non-tertiary alcohols as terminal reductants (Scheme 1 A-B).[6] Although $ABTS^{\bullet-}$ is not found in biological systems, it is an ideal radical substrate because its oxidizing power ($ABTS^{\bullet-}/ABTS^{2-}$ $E_{1/2} = +0.68$ V vs. NHE)[7] is comparable to radicals generated during biological oxidative stress (for example, $E^{\circ\prime} = 1.6$ V for $RO^{\bullet}$, 1.0 V for $ROO^{\bullet}$, 0.92 V for Cys-S$^{\bullet}$, and so forth)[8] and its high absorptivity ($1.5 \times 10^4\ M^{-1}\,cm^{-1}$)[9] permits quantification at lower concentrations than would be achievable with $O_2^{\bullet-}$ or H_2O_2.[10] No $ABTS^{\bullet-}$ reduction occurred with **Ru1** alone if either the O–H or C–H group of a CH–OH moiety was absent, or in pure H_2O solutions, which is consistent with alcohol oxidation by β-hydride elimination from a Ru-alkoxide. A similar process has been proposed for the aerobic oxidation of alcohols catalyzed by Ru-oxide/hydroxide materials, in which the resulting Ru-H intermediate reacts with O_2, the terminal oxidant, by 1,2-insertion (Scheme 1 C, top).[11]

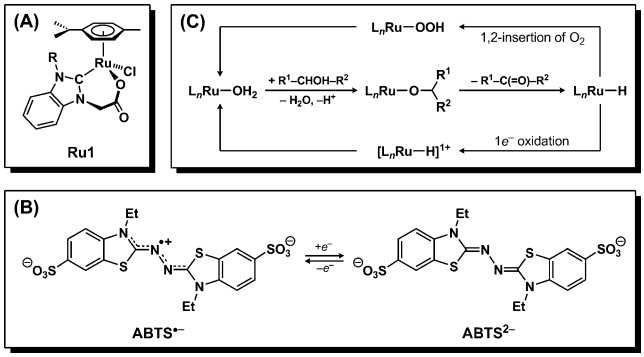

Scheme 1. A) Structure of **Ru1**. B) 1 e^- interconversion between $ABTS^{\bullet-}$ and $ABTS^{2-}$. C) Formation of Ru-hydride in catalytic aerobic alcohol oxidation (top) and $ABTS^{\bullet-}$ reduction (bottom).

If a Ru complex can oxidize a biomolecule to yield a Ru-H species, and if that Ru-H species can then be oxidized by O_2 to yield H_2O_2, then that Ru complex can exert catalytic pro-oxidant effects in biological systems, which has been shown to result in potent anticancer properties by Sadler et al.[12] Compounds such as *trans*-[$RuCl_4$(imidazole)(*S*-dmso)]

[*] Y. Htet, Prof. A. G. Tennyson
Department of Chemistry, Clemson University
Clemson, SC 29634 (USA)
E-mail: atennys@clemson.edu
Prof. A. G. Tennyson
Department of Materials Science and Engineering
Clemson University, Clemson, SC 29634 (USA)
Prof. A. G. Tennyson
Center for Optical Materials Science and Engineering Technologies
91 Technology Drive, Anderson, SC 29625 (USA)

Supporting information for this article can be found under: http://dx.doi.org/10.1002/anie.201601887.

(NAMI-A), and related coordination complexes that also possess anticancer properties, have similarly been shown to function by exertion of pro-oxidant effects.[13] Antioxidant effects have been observed with some Ru coordination complexes, but none exhibited catalytic antioxidant activity.[14] Inspired by the fact that 1) a single Mn porphyrin-based complex can produce either antioxidant or pro-oxidant effects in different environments through a conserved catalytic cycle and set of intermediates and, 2) a catalytic cycle involving a Ru-H intermediate can produce pro-oxidant effects, we hypothesized that a comparable catalytic cycle and Ru-H intermediate could also give rise to antioxidant effects. Herein, we present mechanistic evidence indicating that catalytic antioxidant effects by **Ru1** in the form of catalytic radical reduction (Scheme 1C, bottom) are derived from a similar catalytic cycle and Ru-H intermediate previously shown to produce catalytic pro-oxidant effects.

An organoruthenium-chloride complex and the corresponding aquo complex exist in an equilibrium in H_2O solution that is determined by the relative ligand affinities and total Cl^- ion concentration, but ligand exchange is rapid for both the aquation and anation reactions.[15] Therefore, the Cl^- ligand in **Ru1** will be similarly labile toward substitution with other ligands in phosphate-buffered saline (PBS) solutions, such as $ABTS^{2-}$, H_2O, and EtOH. The chemical synthesis of $ABTS^{\bullet-}$ from $ABTS^{2-}$ does not reach 100% completion,[9] therefore an additional 100 μM of $ABTS^{2-}$ was included to control the variation in rates caused by unreacted $ABTS^{2-}$. Addition of 5 μM of **Ru1** to an aqueous solution containing 100 μM of $ABTS^{2-}$ will result in rapid ligand exchange (relative to turnover) to afford $[L_n\text{Ru-A}_{red}]^{1-}$ and begin the catalytic cycle (Scheme 2). Substitution of $ABTS^{2-}$ by H_2O will yield $[L_n\text{Ru-OH}_2]^{1+}$ (step 1), which will undergo ligand exchange with EtOH to produce $[L_n\text{Ru-(EtOH)}]^{1+}$ (step 2). Complexes similar to $[L_n\text{Ru-OH}_2]^{1+}$ exhibit pK_a values > 9,[16] therefore $[L_n\text{Ru-OH}_2]^{1+}$ is expected to be the predominant form at pH 7.4 rather than $[L_n\text{Ru-OH}]$. Proton transfer from the EtOH ligand to the buffered solution will form $[L_n\text{Ru-OEt}]$ (step 3). Subsequent β-hydride elimination from the ethoxide ligand (via **TS4**) and acetaldehyde dissociation will afford the catalytically active $[L_n\text{Ru-H}]$ intermediate (step 4). This Ru^{II}-hydride species will then undergo 1 e^- oxidation by $ABTS^{\bullet-}$ to yield a Ru^{III}-hydride cation (step 5). Deprotonation by buffer, oxidation by a second equivalent of $ABTS^{\bullet-}$, and subsequent coordination of $ABTS^{2-}$ to Ru, will regenerate $[L_n\text{Ru-A}_{red}]^{1-}$ and restart the cycle (dashed arrow, Scheme 2).

To elucidate the steps in the catalytic cycle, we conducted rate law studies by varying the initial concentration of $ABTS^{\bullet-}$, $ABTS^{2-}$, EtOH, and **Ru1**, as well as solution pH and temperature.[17] The initial rate (v_0) increased linearly with $[ABTS^{\bullet-}]_0$ (Figure 1A), consistent with a reaction that is first-order in $[ABTS^{\bullet-}]$ [Eq. (1)]. This result also suggests that the 2 equiv of $ABTS^{\bullet-}$ per turnover were reduced in separate steps (that is, step 5 followed by the dashed arrow in Scheme 2). A linear relationship is apparent in the plot of k_{obs} versus $1/[ABTS^{2-}]_0$ (Figure 1B), which suggests that $ABTS^{2-}$ dissociation from Ru is necessary for the reaction to proceed (consistent with step 1). An inverse relationship is

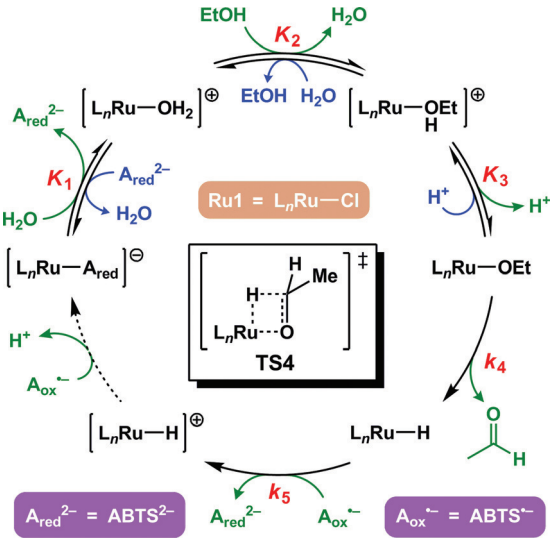

Scheme 2. Proposed mechanism for **Ru1**-catalyzed reduction of $ABTS^{\bullet-}$ into $ABTS^{2-}$, with EtOH as the terminal reductant. Forward reactions (clockwise, green), reverse reactions (counter-clockwise, blue). Each K_n or k_n corresponds to the equilibrium or rate constant, respectively, for the forward reaction in step "n" (step 1 has equilibrium constant K_1, and so forth). The transition-state structure for step 4 is shown as **TS4** in the center. The dashed arrow includes multiple transformations that occur after the rate-determining steps. The spectator ligand set "L_n" comprises the η^6-cymene and κ^2-(C,O)-benzimidazolylidene-carboxylate ligands, but their hapticity/denticity may decrease to accommodate additional ligands.

observed between k_{obs} and $[H^+]$ (Figure 1C), which is expected for H^+ transfer from the EtOH ligand to the (buffered) solution before or during the rate-determining step (consistent with step 3). In contrast, the values of k_{obs} increased as $[EtOH]_0$ increased (Figure 1D), which implies that ligand substitution of the Ru-aquo intermediate by EtOH is a necessary step in the catalytic cycle (consistent with step 2). The plot of k_{obs} versus [**Ru1**] is also linear (Figure 1E), which suggests that the predominant Ru-containing species in solution leading up to the rate-determining step is mononuclear. However, the possibility that multinuclear species were present in solution in minor amounts cannot be definitively excluded. Overall, the rate of $ABTS^{\bullet-}$ reduction is proportionally dependent on $[ABTS^{\bullet-}]_0$, $[EtOH]_0$, and $[\mathbf{Ru1}]_0$, but inversely dependent on $[ABTS^{2-}]_0$ and $[H^+]_0$ [Eq. (2)], which is similar to the rate laws derived by Sigman et al.[18] and Stahl et al.[19] for the Pd- and Cu-catalyzed aerobic oxidation of alcohols.

$$v_0 = -\frac{d[ABTS^{\bullet-}]}{dt} = k_{obs}[ABTS^{\bullet-}] \quad (1)$$

$$-\frac{d[ABTS^{\bullet-}]}{dt} \propto \frac{[EtOH]_0[\mathbf{Ru1}]_0}{[ABTS^{2-}]_0[H^+]_0}[ABTS^{\bullet-}] \quad (2)$$

Plotting $\ln(k_{obs}/T)$ versus $1/T$ (Figure 1F) yields a positive $\Delta S^{\ddagger}$ value (28.9 ± 1.7 cal mol^{-1} K^{-1}), which reveals that disorder increases during the rate-determining step and could arise from ligand dissociation or fragmentation (consistent

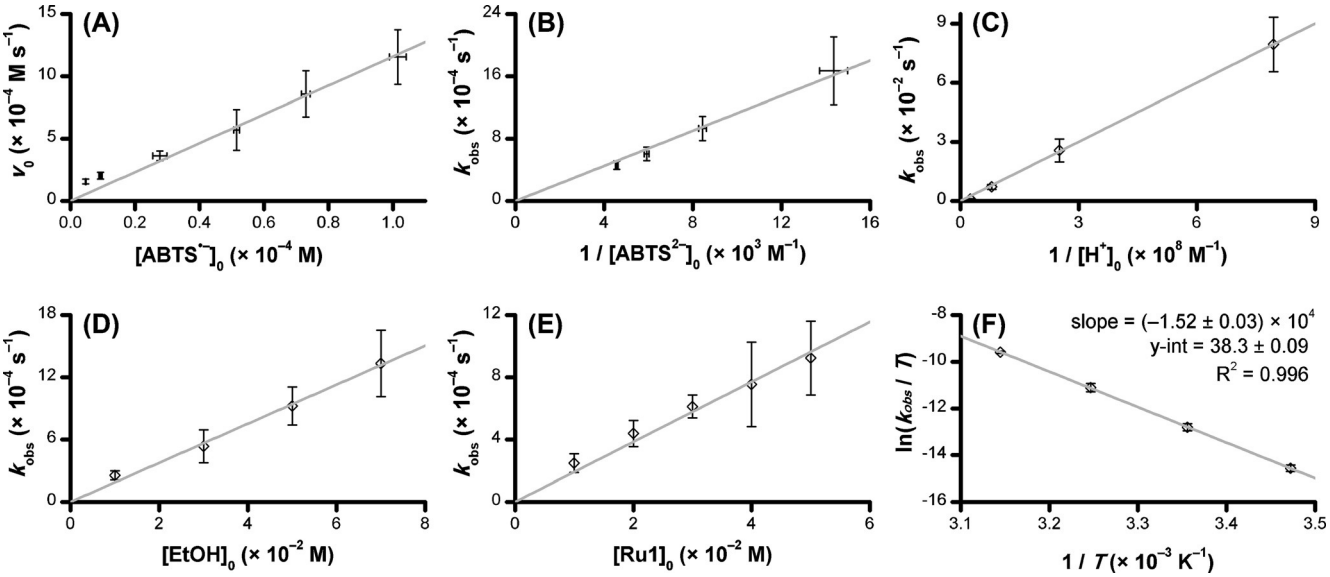

Figure 1. A) Dependence of initial rate (v_0) of **Ru1**-catalyzed ABTS$^{\bullet-}$ reduction on [ABTS$^{\bullet-}$]$_0$ = 5, 10, 25, 50, 75, or 100 μM. Dependence of observed rate constant (k_{obs}) for **Ru1**-catalyzed ABTS$^{\bullet-}$ reduction: B) [ABTS^{2-}]$_0$ = 50, 100, 150, or 200 μM; C) pH 7.4, 7.9, 8.4, or 8.9; D) [EtOH]$_0$ = 10, 30, 50, or 70 mM; E) [**Ru1**]$_0$ = 1, 2, 3, 4, or 5 μM; F) T = 15, 25, 35, or 45 °C. Each data point (◇) is the average of four experiments. Conditions: [**Ru1**]$_0$ = 5 μM, [ABTS$^{\bullet-}$]$_0$ = 50 μM, [ABTS^{2-}]$_0$ = 100 μM, [EtOH]$_0$ = 50 mM, PBS (pH 7.4), 25 °C; absorbance measured at 734 nm.

with **TS4** and step 4). Positive $\Delta S^{\ddagger}$ values were also observed for **Ru1**-catalyzed ABTS$^{\bullet-}$ reduction with *i*-PrOH (32.2 ± 2.3 cal mol^{-1} K^{-1}; Supporting Information, Figure S1), MeOH (11.4 ± 2.9 cal mol^{-1} K^{-1}; Supporting Information, Figure S2), and ethylene glycol (32.8 ± 2.1 cal mol^{-1} K^{-1}; Supporting Information, Figure S3),[17] which suggests that these alcohols also undergo β-hydride elimination (via a **TS4**-like transition state). The presence of acetone did not inhibit the rate of ABTS$^{\bullet-}$ reduction with *i*-PrOH, therefore we conclude that β-hydride elimination with concomitant dissociation of acetone to generate [L$_n$Ru-H] (step 4) is irreversible. A negative $\Delta S^{\ddagger}$ value would be expected if step 5 (a bimolecular reaction) was rate-determining, but v_0 would not vary with [ABTS$^{\bullet-}$]$_0$ if step 4 was rate-determining.[17] Therefore, neither step 4 nor 5 is the unique rate-determining step for the **Ru1**-catalyzed reduction of ABTS$^{\bullet-}$ into ABTS^{2-}. Instead, both steps are likely to exert a comparable influence on catalyst turnover. No ABTS$^{\bullet-}$ reduction occurred with *t*-BuOH, consistent with the inability of [L$_n$Ru-O-*t*-Bu] to undergo β-hydride elimination (step 4 is blocked). This lack of reactivity with *t*-BuOH also suggests that ABTS$^{\bullet-}$ reduction does not occur by oxidation of [L$_n$Ru-OR], because a *t*-BuO$^-$ ligand would render the Ru center more electron-rich, and thus easier to oxidize, than either EtO$^-$ or *i*-PrO$^-$. A similar lack of reactivity with 1,2-dimethoxyethane was unsurprising, given that no [L$_n$Ru-OR] intermediate can be formed (step 3 is blocked).

To confirm that C–H and O–H bond breakage occurred before or during the rate-determining steps, **Ru1**-catalyzed ABTS$^{\bullet-}$ reduction was performed with EtOH, [D$_6$]EtOH, *i*-PrOH, and [D$_8$]-*i*-PrOH, in proteo and deutero PBS.[17] Significantly greater kinetic isotope effects (KIEs) were observed for the C–H/D and O–H/D isotopic substitutions in proteo versus deutero PBS, consistent with the role of H$_2$O in multiple steps of the proposed mechanism: displacement of ABTS^{2-} by H$_2$O (step 1), ligand exchange with EtOH (step 2), and H$^+$ transfer from the EtOH ligand to the buffered solution (step 3). Substituting H$_2$O with D$_2$O can affect the equilibrium for each step, therefore it is unsurprising to observe a solvent KIE for **Ru1**-catalayzed ABTS$^{\bullet-}$ reduction. The solvent KIE values calculated using EtOH and *i*-PrOH as terminal reductants (1.76 ± 0.39 and 1.72 ± 0.37, respectively) were consistent with base-catalyzed H$^+$ transfer (that is not rate-determining) and agreed with previously reported values for catalytic redox reactions involving ABTS$^{\bullet-}$,[20] Ru-mediated alcohol oxidation,[21] and enzymes[22] in H$_2$O and D$_2$O solutions.

The KIEs for the C–H/D and O–H/D isotopic substitutions in EtOH and *i*-PrOH were unambiguous for primary KIEs,[23] which demonstrates that O–H and C–H bond breakage both occurred before or during the rate-determining steps (consistent with step 3 and **TS4**). Notably, the C–H/D KIE values measured for **Ru1**-catalyzed ABTS$^{\bullet-}$ reduction with EtOH (2.88 ± 0.27) and *i*-PrOH (2.86 ± 0.31) were nearly identical to the corresponding C–H/D values reported by Bäckvall et al. (2.57 ± 0.26) and Casey et al. (2.86 ± 0.20) for respective H$_2$ transfers from 1-(4-fluorophenyl)ethanol and *i*-PrOH to other Ru complexes similar to **Ru1**.[24] In contrast, the O–H/D KIE values observed for **Ru1**-catalyzed ABTS$^{\bullet-}$ reduction with EtOH (2.92 ± 0.51) and *i*-PrOH (4.18 ± 0.60) were significantly greater than the corresponding values reported by Bäckvall et al. (1.87 ± 0.17) and Casey et al. (1.79 ± 0.07). One possible cause for this difference is that [L$_n$Ru-H] is formed by H$^+$ transfer from the O–H group in a separate step before β-hydride elimination (that is, step 3 followed by **TS4**), whereas the systems studied by Bäckvall et al. and Casey et al. involved H$_2$ transfer from the CH–OH moiety in a single, concerted step. The slightly

smaller O–H/D KIE value measured for EtOH versus *i*-PrOH with **Ru1** could be due to the greater acidity of EtOH, which lowers the activation barrier to H^+ dissociation and renders ionic O–H bond breakage less sensitive to H/D isotopic substitution.

We propose that $[L_nRu\text{-}H]$ undergoes 1 e^- oxidation by $ABTS^{\bullet-}$ to produce a cationic 17 e^- Ru^{III} complex, $[L_nRu\text{-}H]^{1+}$ (Scheme 3 A). Deprotonation of $[L_nRu\text{-}H]^{1+}$ followed by coordination of an additional ligand L′ from solution (for example, H_2O) generates $[L_nRu\text{-}L']$. This 19 e^- Ru^I complex is oxidized by a second equivalent of $ABTS^{\bullet-}$ and subsequently combines with the resultant $ABTS^{2-}$ to produce $[L_nRu\text{-}A_{red}]^{1-}$ and complete the catalytic cycle. Direct observation of these subsequent steps was not possible because these reactions occurred after the rate-determining steps. However, literature precedent (see below) suggests that the proposed 1 e^- oxidation of $[L_nRu\text{-}H]$ and $[L_nRu\text{-}L']$ by $ABTS^{\bullet-}$, as well as deprotonation of $[L_nRu\text{-}H]^{1+}$ at pH 7.4, is thermodynamically favorable.

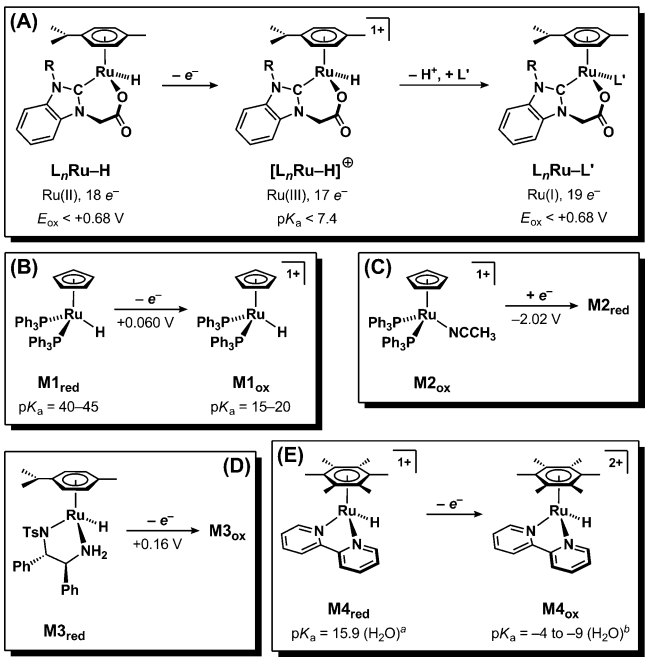

Scheme 3. A) Proposed completion of the catalytic cycle starting from $[L_nRu\text{-}H]$, and B–E) literature precedent. Unless specified otherwise, pK_a values and redox potentials were measured in CH_3CN solutions. [a] pK_a value for $\mathbf{M4_{red}}$ in H_2O estimated using ref. [29]. [b] pK_a value for $\mathbf{M4_{ox}}$ estimated using ref. [25].

Tilset and Norton et al. have shown that $\mathbf{M1_{red}}$ undergoes 1 e^- oxidation at +0.060 V to form $\mathbf{M1_{ox}}$, which has a pK_a 20–25 log units lower than $\mathbf{M1_{red}}$ (Scheme 3 B).[25] Oxidation of $\mathbf{M1_{red}}$ into $\mathbf{M1_{ox}}$ by $ABTS^{\bullet-}$ is expected to be thermodynamically feasible because the $ABTS^{\bullet-}/ABTS^{2-}$ redox couple occurs at +0.68 V.[7] Tilset and Norton et al. also noted that the deprotonation of $\mathbf{M1_{ox}}$ occurs even if it is thermodynamically unfavorable by 4 pK_a units, provided that the 19 e^- Ru^I conjugate base ($\mathbf{M2_{red}}$) is irreversibly oxidized. Even a weak oxidant, such as $[Co(\eta^5\text{-}C_5Me_5)_2]^{1+}$ ($E_{1/2} = -1.51$ V),[26] could oxidize $\mathbf{M2_{red}}$ because the 1 e^- reduction of $\mathbf{M2_{ox}}$ into $\mathbf{M2_{red}}$ occurs at −2.02 V (Scheme 3 C).[25a] Oxidation of the 19 e^- Ru^I intermediate $[L_nRu\text{-}L']$ (analogous to $\mathbf{M2_{red}}$) by $ABTS^{\bullet-}$ should be similarly favorable, and would likewise facilitate deprotonation of $[L_nRu\text{-}H]^{1+}$.

An anionic $\eta^5\text{-}C_5H_5$ ligand is more electron-donating than a neutral η^6-cymene, thus it is more relevant to compare the oxidation of $[L_nRu\text{-}H]$ to other Ru complexes with η^6-cymene ligands rather than $\mathbf{M1_{red}}$. Unsurprisingly, the oxidation of $\mathbf{M3_{red}}$ (+0.16 V; Scheme 3 D) occurred at a higher potential than $\mathbf{M1_{red}}$,[27] but still well below the $ABTS^{\bullet-}/ABTS^{2-}$ redox couple. The difference in oxidation potentials between $[L_nRu\text{-}H]$ and $\mathbf{M3_{red}}$ is expected to be smaller than that between $\mathbf{M3_{red}}$ and $\mathbf{M1_{red}}$, therefore $ABTS^{\bullet-}$ should be a sufficiently strong oxidant to oxidize both $[L_nRu\text{-}H]$ and $[L_nRu\text{-}L']$.

The complex most similar to $[L_nRu\text{-}H]^{1+}$ for which a pK_a value has been reported, is $\mathbf{M4_{red}}$ (p$K_a = 22.5 \pm 0.1$ in CH_3CN; Scheme 3 E).[28] The pK_a for $\mathbf{M4_{red}}$ in H_2O can be estimated as 15.9 using Morris' method to estimate acidity in different solvents.[29] However, $\mathbf{M4_{red}}$ is an 18 e^- Ru^{II} species and $[L_nRu\text{-}H]^{1+}$ is a 17 e^- Ru^{III} species, therefore a more relevant comparison would involve $\mathbf{M4_{ox}}$, which has not been reported. Using the observations of Tilset and Norton et al. that 1 e^- oxidation of an 18 e^- Ru^{II} complex typically lowers the pK_a by 20–25 log units,[25] the pK_a for $\mathbf{M4_{ox}}$ in H_2O is estimated to be in the range of −4 to −9. Similarly dramatic decreases in pK_a have been observed following 1 e^- oxidation of $[RuH(\eta^5\text{-}C_5H_5)(CO)(PPh_3)]$ (from 27–28 to 4–5)[30] and $[WH(\eta^5\text{-}C_5H_5)(CO)_2]$ (from 16 to −3).[31] Therefore, $[L_nRu\text{-}H]^{1+}$ should be sufficiently acidic to undergo complete deprotonation in pH 7.4 aqueous solution.

In summary, mechanistic data for the catalytic reduction of $ABTS^{\bullet-}$ into $ABTS^{2-}$ by **Ru1**, with EtOH as the terminal reductant, suggests that β-hydride elimination from a Ru-alkoxide species generates the catalytically active Ru-H intermediate. In light of previous reports indicating that, 1) Ru-H intermediates can achieve anticancer properties by exerting catalytic pro-oxidant effects,[12] and 2) some Mn porphyrin-based complexes can produce catalytic antioxidant or pro-oxidant effects in different environments with distinct therapeutic uses,[3–5] we believe that new therapeutic strategies and applications can potentially be developed that utilize the catalytic radical reducing ability we have demonstrated for complexes that form Ru–hydride intermediates.

Acknowledgements

This work was supported by the National Science Foundation (DMR-1555224). We thank Dr. A. Mangalum for prior work with **Ru1** and helpful discussions.

Keywords: carbene ligands · dehydrogenation · electron transfer · radical reactions · ruthenium

How to cite: *Angew. Chem. Int. Ed.* **2016**, *55*, 8556–8560
Angew. Chem. **2016**, *128*, 8698–8702

[1] a) M. J. Murphy, *Biochem. J.* **2009**, *417*, 1 – 13; b) M. Valko, D. Leibfritz, J. Moncol, M. T. D. Cronin, M. Mazur, J. Telser, *Int. J. Biochem. Cell Biol.* **2007**, *39*, 44 – 84.

[2] J. Nordberg, E. S. J. Arnér, *Free Radical Biol. Med.* **2001**, *31*, 1287 – 1312.

[3] a) I. Batinic-Haberle, A. Tovmasyan, I. Spasojevic, *Redox Biol.* **2015**, *5*, 43 – 65; b) I. Batinic-Haberle, A. Tovmasyan, E. R. H. Roberts, Z. Vujaskovic, K. W. Leong, I. Spasojevic, *Antioxid. Redox Signaling* **2014**, *20*, 2372 – 2415; c) S. Miriyala, I. Spasojevic, A. Tovmasyan, D. Salvemini, Z. Vujaskovic, D. St. Clair, I. Batinic-Haberle, *Biochim. Biophys. Acta Mol. Basis Dis.* **2012**, *1822*, 794 – 814; d) I. Batinic-Haberle, Z. Rajic, A. Tovmasyan, J. S. Reboucas, X. Ye, K. W. Leong, M. W. Dewhirst, Z. Vujaskovic, L. Benov, I. Spasojevic, *Free Radical Biol. Med.* **2011**, *51*, 1035 – 1053; e) I. Batinić-Haberle, J. S. Rebouças, I. Spasojević, *Antioxid. Redox Signaling* **2010**, *13*, 877 – 918; f) S. R. Doctrow, K. Huffman, C. B. Marcus, G. Tocco, E. Malfroy, C. A. Adinolfi, H. Kruk, K. Baker, N. Lazarowych, J. Mascarenhas, B. Malfroy, *J. Med. Chem.* **2002**, *45*, 4549 – 4558.

[4] a) A. Tovmasyan, R. S. Sampaio, M.-K. Boss, J. C. Bueno-Janice, B. H. Bader, M. Thomas, J. S. Reboucas, M. Orr, J. D. Chandler, Y.-M. Go, D. P. Jones, T. N. Venkatraman, S. Haberle, N. Kyui, C. D. Lascola, M. W. Dewhirst, I. Spasojevic, L. Benov, I. Batinic-Haberle, *Free Radical Biol. Med.* **2015**, *89*, 1231 – 1247; b) M. K. Evans, A. Tovmasyan, I. Batinic-Haberle, G. R. Devi, *Free Radical Biol. Med.* **2014**, *68*, 302 – 314; c) S. D. Amaral, B. P. Espósito, *Biometals* **2008**, *21*, 425 – 432.

[5] a) R. Kubota, S. Imamura, T. Shimizu, S. Asayama, H. Kawakami, *ACS Med. Chem. Lett.* **2014**, *5*, 639 – 643; b) M. A. Sharpe, R. Olloson, V. C. Stewart, J. B. Clark, *Biochem. J.* **2002**, *366*, 97 – 107; c) M. Itoh, K.-i. Motoda, K. Shindo, T. Kamiusuki, H. Sakiyama, N. Matsumoto, H. Ōkawa, *J. Chem. Soc. Dalton Trans.* **1995**, 3635 – 3641; d) Y. Naruta, K. Maruyama, *J. Am. Chem. Soc.* **1991**, *113*, 3595 – 3596.

[6] Y. Htet, A. G. Tennyson, *Chem. Sci.* **2016**, DOI: 10.1039/C1036SC00651E.

[7] S. L. Scott, W.-J. Chen, A. Baka, J. H. Espenson, *J. Phys. Chem.* **1993**, *97*, 6710 – 6714.

[8] a) All redox potentials are reported relative to NHE unless specified otherwise; b) U. Jungwirth, C. R. Kowol, B. K. Keppler, C. G. Hartinger, W. Berger, P. Heffeter, *Antioxid. Redox Signaling* **2011**, *15*, 1085 – 1127.

[9] R. Re, N. Pellegrini, A. Proteggente, A. Pannala, M. Yang, C. Rice-Evans, *Free Radical Biol. Med.* **1999**, *26*, 1231 – 1237.

[10] a) Achieving the same absorbance value as $ABTS^{\bullet-}$ requires a 7.9-fold higher concentration of $O_2^{\bullet-}$ ($\varepsilon = 1.9 \times 10^3\,M^{-1}cm^{-1}$ at 250 nm) or a 344-fold higher concentration of H_2O_2 ($\varepsilon = 43.6\,M^{-1}cm^{-1}$ at 240 nm); b) B. H. J. Bielski, A. O. Allen, *J. Phys. Chem.* **1977**, *81*, 1048 – 1050; c) K. Yusa, K. Shikama, *Biochemistry* **1987**, *26*, 6684 – 6688.

[11] a) F. Nikaidou, H. Ushiyama, K. Yamaguchi, K. Yamashita, N. Mizuno, *J. Phys. Chem. C* **2010**, *114*, 10873 – 10880; b) K. Yamaguchi, N. Mizuno, *Angew. Chem. Int. Ed.* **2002**, *41*, 4538 – 4542; *Angew. Chem.* **2002**, *114*, 4720 – 4724.

[12] a) J. J. Soldevila-Barreda, I. Romero-Canelón, A. Habtemariam, P. J. Sadler, *Nat. Commun.* **2015**, *6*, 6582; b) Y. Fu, M. J. Romero, A. Habtemariam, M. E. Snowden, L. Song, G. J. Clarkson, B. Qamar, A. M. Pizarro, P. R. Unwin, P. J. Sadler, *Chem. Sci.* **2012**, *3*, 2485 – 2494; c) S. J. Dougan, A. Habtemariam, S. E. McHale, S. Parsons, P. J. Sadler, *Proc. Natl. Acad. Sci. USA* **2008**, *105*, 11628 – 11633.

[13] a) M. Vadori, C. Florio, B. Groppo, M. Cocchietto, S. Pacor, S. Zorzet, L. Candussio, G. Sava, *J. Biol. Inorg. Chem.* **2015**, *20*, 831 – 840; b) H. Hu, Y. You, L. He, T. Chen, *J. Mater. Chem. B* **2015**, *3*, 6338 – 6346; c) B. Fischer, P. Heffeter, K. Kryeziu, L. Gille, S. M. Meier, W. Berger, C. R. Kowol, B. K. Keppler, *Dalton Trans.* **2014**, *43*, 1096 – 1104.

[14] a) B. R. Cameron, M. C. Darkes, H. Yee, M. Olsen, S. P. Fricker, R. T. Skerlj, G. J. Bridger, N. A. Davies, M. T. Wilson, D. J. Rose, J. Zubieta, *Inorg. Chem.* **2003**, *42*, 1868 – 1876; b) S. P. Fricker, E. Slade, N. A. Powell, O. J. Vaughan, G. R. Henderson, B. A. Murrer, I. L. Megson, S. K. Bisland, F. W. Flitney, *Br. J. Pharmacol.* **1997**, *122*, 1441 – 1449.

[15] a) H. Chen, J. A. Parkinson, R. E. Morris, P. J. Sadler, *J. Am. Chem. Soc.* **2003**, *125*, 173 – 186; b) L. Dadci, H. Elias, U. Frey, A. Hörnig, U. Koelle, A. E. Merbach, H. Paulust, J. S. Schneider, *Inorg. Chem.* **1995**, *34*, 306 – 315.

[16] a) A. F. A. Peacock, M. Melchart, R. J. Deeth, A. Habtemariam, S. Parsons, P. J. Sadler, *Chem. Eur. J.* **2007**, *13*, 2601 – 2613; b) R. Fernández, M. Melchart, A. Habtemariam, S. Parsons, P. J. Sadler, *Chem. Eur. J.* **2004**, *10*, 5173 – 5179.

[17] For experimental details, supplementary data plots, and equation derivations, see the Supporting Information.

[18] a) J. A. Mueller, A. Cowell, B. D. Chandler, M. S. Sigman, *J. Am. Chem. Soc.* **2005**, *127*, 14817 – 14824; b) M. J. Schultz, R. S. Adler, W. Zierkiewicz, T. Privalov, M. S. Sigman, *J. Am. Chem. Soc.* **2005**, *127*, 8499 – 8507.

[19] a) S. D. McCann, S. S. Stahl, *J. Am. Chem. Soc.* **2016**, *138*, 199 – 206; b) J. M. Hoover, B. L. Ryland, S. S. Stahl, *J. Am. Chem. Soc.* **2013**, *135*, 2357 – 2367.

[20] R. Panicucci, T. C. Bruice, *J. Am. Chem. Soc.* **1990**, *112*, 6063 – 6071.

[21] E. P. Kelson, P. P. Phengsy, *Int. J. Chem. Kinet.* **2000**, *32*, 760 – 770.

[22] a) A. J. Nicoll, R. K. Allemann, *Org. Biomol. Chem.* **2004**, *2*, 2175 – 2180; b) J. H. Kim, M. G. Ryan, H. Knaut, R. Hille, *J. Biol. Chem.* **1996**, *271*, 6771 – 6780; c) G. R. Bishop, V. L. Davidson, *Biochemistry* **1995**, *34*, 12082 – 12086.

[23] M. Gómez-Gallego, M. A. Sierra, *Chem. Rev.* **2011**, *111*, 4857 – 4963.

[24] a) J. B. Johnson, J.-E. Bäckvall, *J. Org. Chem.* **2003**, *68*, 7681 – 7684; b) C. P. Casey, J. B. Johnson, *J. Org. Chem.* **2003**, *68*, 1998 – 2001.

[25] a) K.-T. Smith, M. Tilset, S. S. Kristjánsdóttir, J. R. Norton, *Inorg. Chem.* **1995**, *34*, 6497 – 6504; b) K.-T. Smith, C. Rømming, M. Tilset, *J. Am. Chem. Soc.* **1993**, *115*, 8681 – 8689.

[26] N. G. Connelly, W. E. Geiger, *Chem. Rev.* **1996**, *96*, 877 – 910.

[27] K. R. Brownell, C. C. L. McCrory, C. E. D. Chidsey, R. H. Perry, R. N. Zare, R. M. Waymouth, *J. Am. Chem. Soc.* **2013**, *135*, 14299 – 14305.

[28] Y. Matsubara, E. Fujita, M. D. Doherty, J. T. Muckerman, C. Creutz, *J. Am. Chem. Soc.* **2012**, *134*, 15743 – 15757.

[29] R. H. Morris, *J. Am. Chem. Soc.* **2014**, *136*, 1948 – 1959.

[30] O. B. Ryan, M. Tilset, V. D. Parker, *Organometallics* **1991**, *10*, 298 – 304.

[31] O. B. Ryan, M. Tilset, V. D. Parker, *J. Am. Chem. Soc.* **1990**, *112*, 2618 – 2626.

Received: February 23, 2016
Revised: April 3, 2016
Published online: June 2, 2016

